Check for
updates

HHLA2 deficiency inhibits pancreatic cancer progression and THP-1 macrophage M2 polarization via EGFR/MAPK/ERK and mTOR/AKT pathway

Siqi Zhou[1,2†], Zhangding Wang[2†], Dian Zhao[3†], Yao Fu[4], Shu Zhang[1,2*], Zhiping Wang[5*] and Xiaoping Zou[1,2*]

Abstract

Background Human endogenous retrovirus subfamily H long terminal repeat associating protein 2, (HHLA2), a member of B7 family, exhibits heightened expression in various malignant tumors. However, the exact functions of HHLA2 in pancreatic cancer (PC) remain incompletely elucidated.

Methods We initially conducted an analysis of the B7 family members' expression pattern in pancreatic tumor samples and adjacent normal tissues using The Cancer Genome Atlas (TCGA) database. Subsequently, immunohistochemistry, RT-qPCR and western blot methods were used to assess HHLA2 expression levels in PC tissues and cell lines. Furthermore, after silencing HHLA2 in PC cell lines, cell migration and proliferation of PC cells were detected by wound healing and CCK-8 assays, and cell invasion of PC cells was detected by transwell assays. We also investigated the regulation of epithelial-mesenchymal transition (EMT) markers and levels of EGFR, MEK, ERK1/2, mTOR and AKT via western blot analysis. Finally, the correlation between HHLA2 expression and immune infiltration was further explored.

Results Silencing of HHLA2 resulted in the inhibition of PC cell proliferation, migration and invasion, potentially through the suppression of the EGFR/MAPK/ERK and mTOR/AKT signaling pathway. Additionally, silencing HHLA2 led to the inhibition of M2-type polarization of tumor associated macrophages (TAMs).

Conclusion The knockdown of HHLA2 was observed to inhibit the migration and invasion of PC cells through the regulation of the EMT process and EGFR/MAPK/ERK and mTOR/AKT pathway. Furthermore, silencing HHLA2 was found to modulate M2 polarization of TAMs. These finding suggest that HHLA2 could be a promising therapeutic target for Pancreatic cancer.

Keywords Pancreatic cancer, HHLA2, Tumor-associated macrophages, Migration, Invasion

---

†Siqi Zhou, Zhangding Wang and Dian Zhao contributed equally to this work.

*Correspondence:
Shu Zhang
zhangsgastro@nju.edu.cn
Zhiping Wang
zhpsqxt@163.com
Xiaoping Zou
zouxp@nju.edu.cn
Full list of author information is available at the end of the article

Introduction

Pancreatic cancer (PC) is one of the most aggressive malignant tumors and known as 'king of cancer' [1, 2]. The incidence of PC ranks the eighth among all malignant tumors in China, and it is the seventh cause of cancer related death worldwide. Pancreatic ductal adenocarcinoma is predicted to become the second cause of cancer-related death in the next 20 years. The pancreas is located at the posterior side of the upper abdomen, which is easy to be ignored. Therefore, the early diagnosis of PC is difficult, and more than 80% of the first-diagnosed patients were at the advanced stage. Only 10% of patients with PC are suitable for surgery, and the risk of postoperative metastasis is also high, and patients with recurrence of PC are often highly resistant to radio and chemotherapies. Due to the lack of effective treatments, the 5-year survival rate of PC is less than 9% [3]. Therefore, results of current studies suggested that by regulating the composition of extracellular matrix, reactivation of the antitumor environment in PC may improve the therapeutic efficacy of current treatment resistance and benefit the patients [4].

Immune checkpoint plays an important role in the immune escape of tumor cells [5, 6]. Therapeutic strategies that inhibit the immune checkpoint signaling have been widely used in the treatment of PC. At present, the commonly analyzed immune checkpoint proteins mainly include cytotoxic T lymphocyte-associated antigen-4 (CTLA-4), programmed death receptor-1 (PD-1) and its ligands (PD-L1) [7, 8]. However, the therapeutic efficacy of immune checkpoints for the treatment of PC remains unclear. In a phase II clinical trial, 27 patients with PC did not respond to the treatment of anti-CTLA-4 monoclonal antibody Ipilimumab [9]; in another phase I trial using anti-PD-L1 monoclonal antibody, 14 patients with PC showed disappointing responses to the monotherapy [10]. Therefore, exploring additional immune checkpoint markers and developing adequate immune classifications to improve the efficacy of current anti-PC therapies is critical.

The B7 family proteins belong to the immunoglobulin superfamily (IgSF). The molecular structure of B7 family proteins is similar to that of the immunoglobulins. Each motif domain of B7 family proteins is a tightly folded structure composed of 70 to 110 amino acids, including IgV region and IgC2 region [11–13]. It is expressed as a single chain on the surface of antigen presenting cells (APCs) and acts as a second signal of immune response by binding to CD28 through IgV region [14]. B7 family members include B7-1 (CD80), B7-2 (CD86), B7-H1/PD-L1(CD274), ICOS-L/B7-H2(CD275), B7-H3(CD276), B7-H4, B7-DC/PD-L2(CD273), BT3.1(CD277) and the new member B7H7, which is also known as human endogenous retrovirus subfamily H long terminal repeat associating protein 2(HHLA2) [15]. uwhich is longer than most B7 family members. It is speculated that the HHLA2 protein contains an N-terminal signal peptide, which is mainly localized at the cell membranes and intracellular regions of different cells [16–18]. HHLA2 can activate TCR signaling and decrease the proliferation of the CD4 and CD8 cells, thereby decreased the production of IFN-γ, TNF-α, IL-5, IL-10, IL-13, L-17 A and IL-22 and reduced the immune responses [19, 20]. Results of previous studies suggested that HHLA2 may serve as a new immune checkpoint molecule for the development tumor and participate in the process of tumor immune escape, and provide opportunities for the survival of tumor cell [21]. However, the underlying mechanism remains unclear.

At present, there are few reports focused on the roles and mechanisms of HHLA2 in PC. In this study, we detected the expression of HHLA2 in PC tissues, performed cell studies and also used bioinformatics to explore the roles of HHLA2 in PC. We hypothesized that HHLA2 is over-expressed in PC and may facilitate the development of the tumor.

Materials and methods

Public data information

We retrieved transcriptome RNA expression data and corresponding clinical information of 345 PC patients from TCGA (The Cancer Genome Atlas) (http://cancergenome.nih.gov/) database. Inclusion criteria: confirmed PC diagnosis, availability of complete gene expression profiles, and comprehensive prognostic follow-up data. We employed the limma and SVA packages to homogenize the transcriptome data from various genes, and the combined database was referred to as Merge database. Subsequently, E-MTAB-5639 consisting RNA-seq on subcutaneous PDTXs from 24 PDAC samples, was used to verify the differentially expressed genes (DEGs) between different HHLA2-expression groups. To assess immune cell infiltration in PC tumor tissues, TIMER (Tumor Immune Estimation Resource) (http://timer.cistrome.org/) database was utilized to determine the infiltration of immune cells in tumor tissues TIMER provide valuable information regarding the infiltration of B cells, CD4 + T cells, CD8 + T cells, neutrophils, macrophages and dendritic cells, offering insights into the immune landscape of PC.

Human specimens

Sixty-two PC tissues and adjacent normal pancreas were collected at the affiliated Drum Tower Hospital of Nanjing University Medical School. Writing informed consent was acquired from the donors. The study was

Zhou *et al. World Journal of Surgical Oncology*   (2024) 22:133

Page 3 of 13

approved by the Institutional Ethics Review Board of the affiliated Drum Tower Hospital of Nanjing University Medical School.

Cell lines and reagents

Human normal Pancreatic Duct Epithelial cell line (HPDE), human pancreatic cancer cell lines (BxPC-3 CFPAC-1, Capan-2, PANC-1, HPAC, AsPC-1, MIA-PaCa-2 and SW1990) were purchased from American Type Culture Collection (American Type Culture Collection cell line bank, Manassas, VA, USA). DMEM medium and fetal bovine serum was purchased from Gibco (USA). HHLA2 siRNA and negative control siRNA (NC siRNA) plasmids were designed and synthesized by Genepharma (Shanghai, China). Transfection reagent Lipofectamine 2000 was purchased from Thermo Fisher (San Jose, CA, USA). DAB chromogen was purchased from Sangon (Shanghai, China).

Cell culture

Cells were cultured in DMEM medium containing 10% FBS fetal bovine serum at 37℃ in a 5% CO_2 environment. The cells were digested and passaged when reached about 80% confluency. For the cell passage, the cells were digested with trypsin and then collected by centrifugation. Cells were then resuspended in fresh medium, and the cell suspension was ready to seed plates as required for subsequent experiments.

Survival analysis

The expression and clinical data of B7 family members including CD274, CD276, CD80, CD86, HHLA2, ICOSLG, NCR3LG1, PDCD1LG2, VSIR and VTVN1 in PC patients were analyzed. According to the expression levels of B7 family members, the first 30% and the last 30% were set as high expression group and the low expression group, respectively. Kaplan-Meier analysis was used to compare the survival rate of PC patients between high and low expression of B7 family members.

Immunohistochemistry

Clinical specimens of PC were fixed in 10% formalin and encapsulated in paraffin blocks. 5-μm sections were cut and mounted on slides. Samples were blocked with 5% goat serum for 1 h at room temperature, followed by incubation with the primary antibodies (1:200) overnight at 4℃. After washing twice with PBS, rabbit secondary antibodies (1:200) were incubated for 2 h at room temperature. Then, 3, 3' diaminobenzidine (DAB) was used for coloration, hematoxylin counterstained, dehydration and sealing. Sections incubated with goat serum without the primary antibody served as negative controls.

Colony-formation assay

PC cells transfected with siRNA were counted and seeded into 6-well plates with 1000 cells/well. After 14 days, the cells were fixed in methanol and colonies were counted after staining with 0.1% crystal violet in 25% methanol for 20 min. The results were presented as the average number of counted colonies per well under each condition. All the experiments were performed in triplicate and repeated three times independently.

Wound healing assay

Cells were seeded onto 6-well plates at a density of 5×10^5 cells/well and cultured overnight in an incubator. After the cells were covered with the culture plate, the tip of a 20 μl pipette gun was used to scratch the cell monolayer perpendicular to the plate, with an interval of 0.5 ~ 1 cm. After washing the cells with PBS for 3 times, the medium containing 2% FBS and siHHLA2-2 and siHHLA2-3 were added, and then the cells were cultured in an incubator. Measurements were taken at the same location after 0 h and 24 h of culture, and three compound wells were measured each time and repeated three times. Scratch width was measured using Image J. Wound healing rate= (0 h scratch width- 24 h scratch width)/ 0 h scratch width ×100%.

Transwell assay

Cellular motility and invasive abilities were determined using Transwell (8.0 μm polycarbonate Membrane, Corning Life Sciences, Bedford, MA, USA) and Matrigel invasion (BD Biosciences, San Jose, CA, USA), respectively. For the cell invasion analysis, transwell chambers were placed on 24-well plates; the upper chamber coated with Matrigel was seeded with 2×10^5 cells and cultured with 200 μl serum-free medium, and the lower chamber was added with 600 μl DMEM medium containing 10% FBS. After 24 h of culture, the chambers were removed and fixed with 4% paraformaldehyde at room temperature for 20 min, and then stained with crystal violet at room temperature for 15 min. The cells in the upper chamber were gently wiped off with a cotton swab. Five fields were randomly selected under a microscope and photographed (200×), Image J software was used for cell counting. The migration experiments were performed in the same manner, but the upper chamber was without the Matrigel.

Western blot

Total protein was extracted from cell samples, and protein concentration was determined by BCA assay. Proteins were then denatured by boiling with 20 μg protein loading buffer and wet transferred to nitrocellulose membrane after gel electrophoresis on 10%SDS-PAGE,

Zhou *et al. World Journal of Surgical Oncology*   (2024) 22:133

Page 4 of 13

blocked with 5% skim milk powder for 1 h at room temperature. After addition of primary antibodies (1:1000), the membranes were incubated overnight at 4 ℃, washed, and the secondary antibodies (1:2000) were added and incubated for 2 h at room temperature., Then the membranes were washed, and chromogen was added. Protein bands were visualized using a chemiluminescence imaging system.

Functional enrichment and Immuno-infiltration analysis
The GO (Gene Ontology) enrichment analysis was performed to determine significantly enriched GO terms for the differentially expressed genes. In order to investigate any changes in biological functions and related pathways, HALLMARK gene set ("H.all.v7.4.symbols.gmt" was downloaded from the Molecular Signatures Database as a reference gene set, http://www.gsea-msigdb.org/gsea/downloads.jsp), and KEGG (Kyoto Encyclopedia of Genes and Genomes) pathway enrichment analysis were performed. Enrichment analysis was performed by the R package clusterProfiler (version 3.14.3). P value of < 0.05 was considered statistically significant. Sangerbox Tools [22] was used to calculate the relationship between each B7 family members and significantly infiltrated immune cells. In addition, TCGA and TIMER2.0 databases were used to analyze the correlation between M2 macrophage infiltration and HHLA2 expression in PC.

Immune correlation analysis of HHLA2
Spearman coefficient was used for evaluating the correlation between HHLA2 and neutrophil and macrophages M2. At the same time, the results were visualized in the form of scatter plots. *P* value < 0.05 was considered as a statistically significant threshold.

THP-1 differentiation and coculture system
To be differentiated into adherent macrophages, THP-1 cells (5×10^5/well) were seeded into 6-well plates in the presence of 100 ng/ml of phorbol 12-myristate 13-acetate (PMA, Sigma) for 24 h. The differentiated macrophages were named as M0 macrophages. To establish a co-culture system, we transfected AsPC-1 and Capan-2 cells with siHHLA2 or NC. At 48 h post-transfection, we used the culture supernatant to incubate the M0 macrophages. After 48 h of co-culture, the macrophages were harvested for analysis.

Statistics analysis
Data were analyzed using SPSS software and GraphPad Prism 7 software. Data are presented as mean ± standard deviation (SD) or 95% confidence intervals. The continuous variables were compared between the two groups by unpaired t test, and the comparison between multiple groups was performed by one-way ANOVA followed by Tukey's test. Categorical variables were compared with the use of the chi-square test or Fisher's exact test, as appropriate. Correlations between two groups were analyzed by the Spearman rank-order correlation analysis. Kaplan-Meier method was used to draw survival curves. *p* < 0.05 was considered to indicate a statistical difference.

Results

Comparison of the expressions of B7 family members between PC tissues and normal tissues
First, we combined the TCGA and the GTEx datasets and analyzed the gene expression data of 178 tumors and 167 normal pancreatic tissues. The results were presented as boxplots (Fig. 1A) and heatmap (Fig. 1B). We found that CD276, CD80, CD86, HHLA2, NCR3LG1 and PDCD1LG2 were significantly elevated, while ICOSLG expression was significantly decreased in PC tissues. And the expression of CD274 has no significant differences between tumor tissues and normal tissues. Additionally, a correlation network plot was used to unravel the correlation features among these 10 B7 family members. Figure 1C showed the correlations between the above genes. Concomitantly, we studied the effects of these 10 B7 family members, age, gender, grade, stage, T/M/N classification and risk score on prognosis of pancreatic cancer. In univariate Cox regression analysis, CD276, CD80, ,VTVN1, CD274and HHLA2 were high-risk factors. The hazard ratio (95% CI) of CD276, CD80, CD274, HHLA2 was 1.451 (1.026,2.050), 2.071 (1.114, 3.851), 1.186 (1.010,1.393), 2.072 (1.341,3.201) and 1.256 (1.062, 1.485), respectively (Fig. 1D). In TCGA dataset, the univariate Cox regression analysis found that age, stage of N and riskScore were significantly associated with survival but the corresponding multivariate Cox regression analysis found that only age and riskScore were significantly associated with survival (HR = 1.296, 95% CI = 1.110–1.513, *p* = 0.001, and HR = 1.253, 95% CI = 1.057–1.485, *p* = 0.009, respectively; Fig. 1E&F).

The expressions of B7 family members were correlated with the survival of PC patients
Next, the potential prognostic values the B7 family members were further evaluated by KM survival analysis based on TCGA datasets. The results showed that high expression of B7 family members in PC predicted poor survival rate. Moreover, increased expression of HHLA2 and PDCD1LG2 were significantly correlated with the unfavorable survival in PC (Fig. 2A-J). Furthermore, we calculated a risk score for each patient based on the gene expression level and the risk coefficient
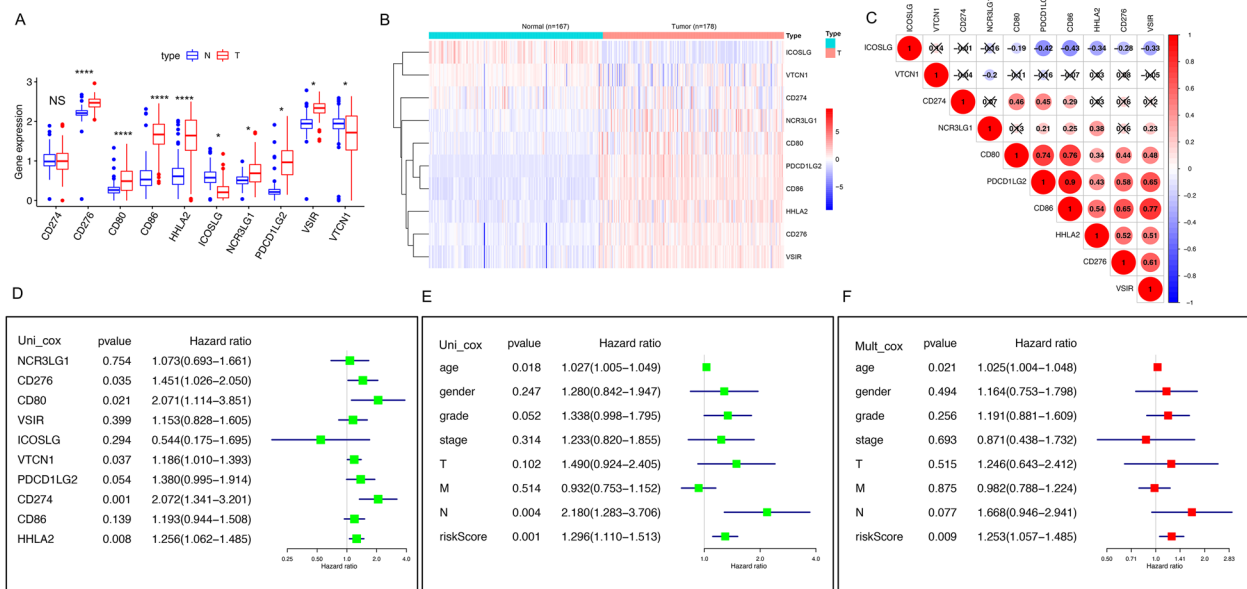
Zhou *et al. World Journal of Surgical Oncology* (2024) 22:133

Page 5 of 13

Fig. 1 The expressions of B7 family members between PC tissues and normal tissues. **A** Expression of B7 family members in pancreatic cancer tissues and normal tissues. **B** Heatmap of B7 family member in normal and cancer tissues (green: low-expression; red: high-expression). **C** Spearman correlation analysis for the 10 types of B7 family members (red: positive correlation; blue: negative correlation). **D** Forest plot of B7 family members by univariate Cox regression analysis. **E**&**F** Univariate and multivariate Cox regression analysis of clinical parameters and risk score

of each gene. The prognostic value of the risk score was assessed by comparing the difference in survival between the high-risk and low-risk groups. In the univariate regression analysis described earlier, we selected 4 high-risk genes CD274, CD276, VTVN1, and HHLA2 and 1 low-risk gene ICOSLG for risk scoring. We plotted the distribution of patients' risk scores and overall survival status as well as the expression profiles of the five genes. As shown in the Fig. 2K, significantly higher mortality and a shorter OS time were observed in the high-risk group. The heatmap showed that the expression levels of VTVN1 and HHLA2 in the low-risk group were lower than high-risk group. Moreover, a heatmap was used to demonstrate the correlation between B7 family members and clinicopathological features in TCGA-PC: that patients in the high-risk group were older and had more lymph node metastases compared to the low-risk group (Fig. 2L).

HHLA2 was over-expressed in PC

Furthermore, the expression of HHLA2 in 6 paired PC tissues and the adjacent normal tissues were detected by WB and RT-qPCR. We found that the expression of HHLA2 in PC tissues was significantly higher than that in adjacent normal tissues (Fig. 3A&B, $p < 0.01$). The IHC staining of tissue samples from 62 PC patients further

verified the HHLA2 protein expression (Fig. 3C). Statistical analysis showed that HHLA2 expression in tumor tissues was significantly higher than that in adjacent normal tissues (Fig. 3D). ($P < 0.05$). In addition, Kaplan–Meier (KM) survival analysis showed that higher expression of HHLA2 was significantly associated with a poor survival outcome in 62 PC patients (Fig. 3G, $p < 0.05$).The protein and mRNA expression levels of HHLA2 were detected in normal ductal epithelial cell line of pancreas and different human pancreatic cancer cell lines by WB and RT-qPCR. Capan-2 and AsPC-1 cells with high expression of HHLA2 were selected for subsequent experiments (Fig. 3E&F, $p < 0.01$).

Relationship between HHLA2 expression and clinic pathological features of PC patients

In the data of 171 PC patients obtained from TCGA database and our self-made paraffin chip (including 62 PC patients), the PC patients were divided into HHLA2 high and low expression groups. As shown in supplemental Table S1, in TCGA database, there was no significant correlation between HHLA2 expression and age, gender, or tumor TNM stage of the patients ($p > 0.05$). In our self-made paraffin chip, we can see that there was significant correlation between HHLA2 expression and overall survival status.
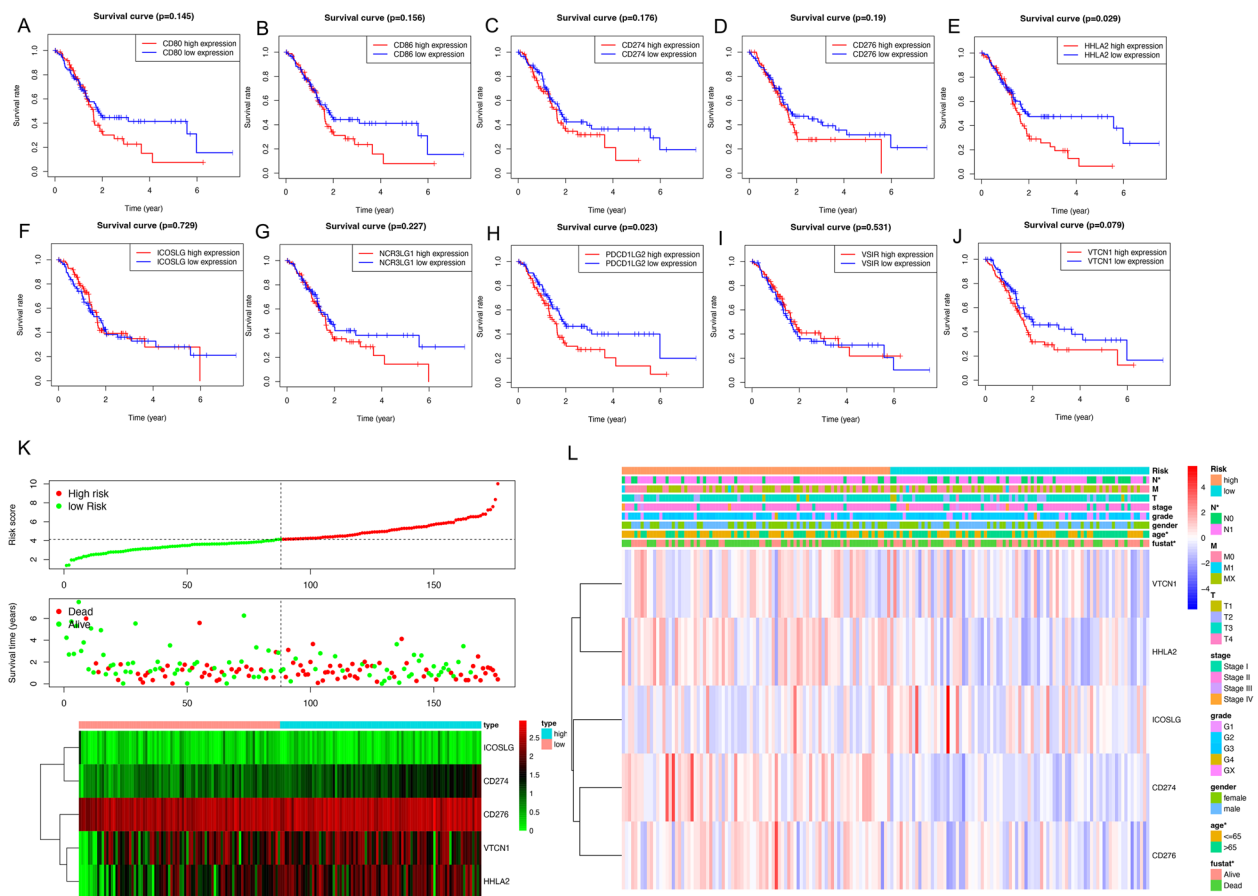
Zhou *et al. World Journal of Surgical Oncology*   (2024) 22:133

Page 6 of 13

Fig. 2 The B7 family members were correlated with the survival of PC patients. **A-J** Survival curves of B7 family members and prognosis of PC; **K** The distribution of risk scores, survival status and heatmap of the selected genes expression levels in datasets of TCGA-PC (left of the dotted line: low-risk population; right of the dotted line: high-risk population; distribution of patients based on the median risk score.) **L** Correlation heatmap of B7 family members and clinicopathological features in datasets of TCGA-PC

Effects of siHHLA2 on viability and proliferation of PC cells

Then, siHHLA2-1, siHHLA2-2 and siHHLA2-3 were transfected into AsPC-1 and Capan-2 cells, and the protein and mRNA expression of HHLA2 was detected by WB and RT-qPCR. Compared with the NC control group, siHHLA2-2 and siHHLA2-3 markedly inhibited the relative expression of HHLA2 in AsPC-1 and Capan-2 cells($p < 0.01$) while siHHLA2-1 showed low inhibitory effects on HHLA2 expression in Capan-2 cells (Fig. 4A&B, $p > 0.05$). Therefore, siHHLA2-2 and siH-HLA2-3 were used in the following studies. The colony formation assay showed that siHHLA2 inhibited the proliferation of AsPC-1 and Capan-2 cells (Fig. 4C, $p < 0.001$). Furthermore, results of CCK-8 suggested that compared with NC group, siHHLA2 significantly inhibited the viability of PC cells AsPC-1 and Capan-2 (Fig. 4D, $p < 0.05$). Furthermore, the immunofluorescence staining demonstrated that after siHHLA2 treatment, the expressions of

Ki67 significantly decreased (Fig. 4E&F, $p < 0.05$). Taken together, these data indicate that knockdown of HHLA2 expression can inhibit the viability of human gastric cancer cells.

Function Enrichment Analysis of HHLA2 in PC

Based on the above, we found that the expression level of HHLA2 was significantly correlated with the proliferative ability of pancreatic cancer cells. However, the signal pathway changes caused by HHLA2 in PC are unknown. In order to deepen the understanding of the functional meaning of HHLA2 in PC, the functional enrichment analysis for HHLA2-related gene sets in PC was performed. We first identified 918 differentially expressed genes (DEGs) between HHLA2-high and HHLA2-low expression groups using the E-MTAB-5639 cohort, of which the HHLA2 high-expression group had 724 up-regulated genes and 194 down-regulated gene expression
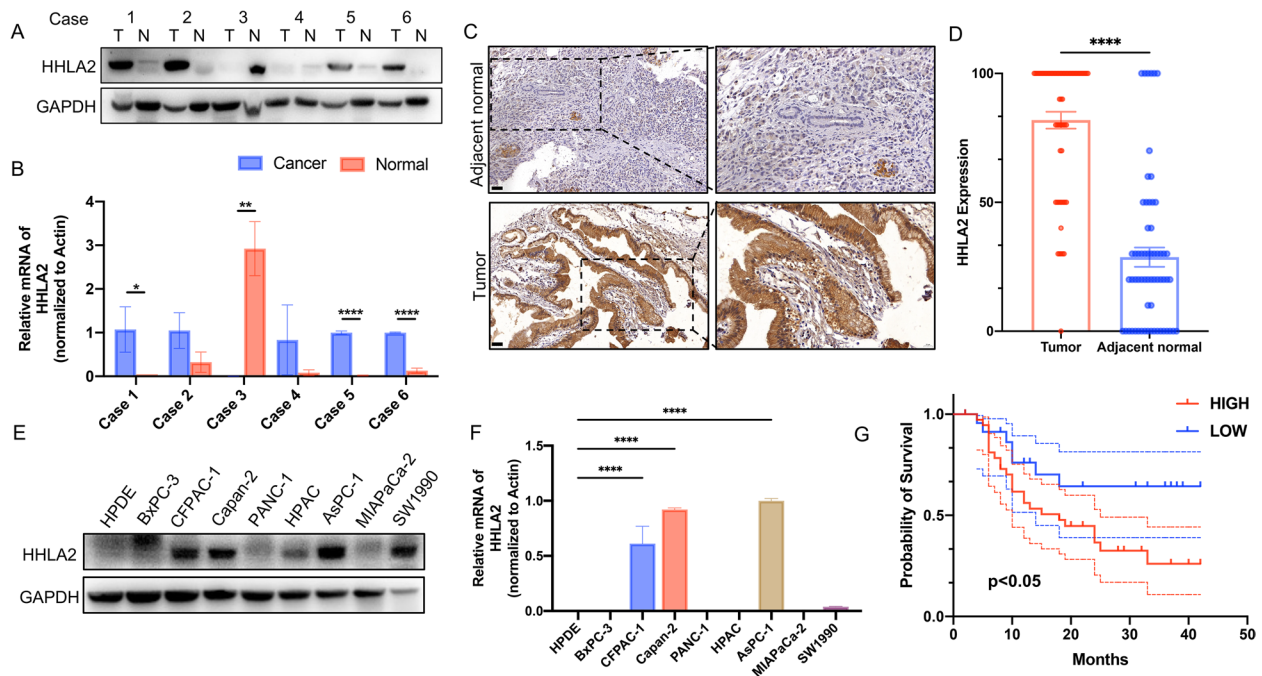
Zhou *et al. World Journal of Surgical Oncology*   (2024) 22:133

Page 7 of 13

Fig. 3 The expression level of HHLA2 in pancreatic cancer tissues and cells. **A** The expression of HHLA2 in pancreatic cancer tissue was detected by WB. **B** The expression of HHLA2 in pancreatic cancer tissue was detected by RT-qPCR. **C**&**D** The expression of HHLA2 in 62 paired adjacent normal tissues and tumor tissues was detected by IHC. Scale bar: 50 μm. **E**&**F** The expression of HHLA2 in pancreatic cancer cells was detected by WB and RT-qPCR. **G** Differential expression of HHLA2 in PC tissues and normal tissues and its survival curve with patients were analyzed. $^{*}p<0.05$, $^{**}p<0.01$, $^{***}p<0.001$, $^{****}p<0.0001$

groups compared to the HHLA2 low-expression group (Fig. 5A&B). KEGG analysis showed that up-regulated genes are involved in Cell adhesion molecules and metabolism-related pathways, including Retinol metabolism, Glycerolipid metabolism, Nitrogen metabolism, and Tyrosine metabolism (Fig. 5C). Hallmark analysis showed correlations with the Inflammatory response and Epithelial Mesenchymal Transition (EMT) pathways (Fig. 5D). GO term analysis showed that upregulated genes were significantly enriched in cell adhesion-related pathways (Fig. 5E). For down-regulated genes, KEGG analysis showed that these genes were involved in the Cytokine-cytokine receptor interaction and EGFR-related signaling pathways such as the ErbB signaling pathway and the Ras signaling pathway (Fig. 5F). Hallmark analysis showed correlation with EMT pathway and Inflammatory response (Fig. 5G), similar to up-regulation genes. GO term analysis also showed that down-regulated genes were enriched during cellular development process and closely related to cell proliferation and epithelium development (Fig. 5H). Above results implied that HHLA2 might be involved in the occurrence and development of PC through EMT pathway and EGFR-related signaling pathway.

Effects of siHHLA2 on the migration and invasion of PC cells

To clarify the effects of HHLA2 on PC cell metastasis, wound healing and transwell assays have been conducted. As shown in Fig. 6A and B, compared with the NC group, the wound healing rate of siHHLA2-2 group and siHHLA2-3 group in AsPC-1 and Capan-2 were significantly decreased after 24 h. Meanwhile, the results of transwell assays indicated that siHHLA2 significantly reduced the number of invaded PC cells (Fig. 6C&D).

Effects of siHHLA2 on mTOR / AKT and EGFR/MAPK/ERK signaling pathway in PC cells

Next, the effects of siHHLA2 on EMT of PC cells were examined. WB and RT-qPCR results showed that the expression of epithelial marker E-cadherin was increased, and the expression of mesenchymal marker vimentin was inhibited by the intervention of siHHLA2 (Fig. 7A&B). EGFR is a cell surface receptor that plays a vital role in regulating tumor metastasis by activating downstream signaling pathways, including the MAPK pathway and the PI3K/Akt pathway. Then, we examined the phosphorylation levels of ERK1/2, MEK, EGFR, AKT and mTOR.
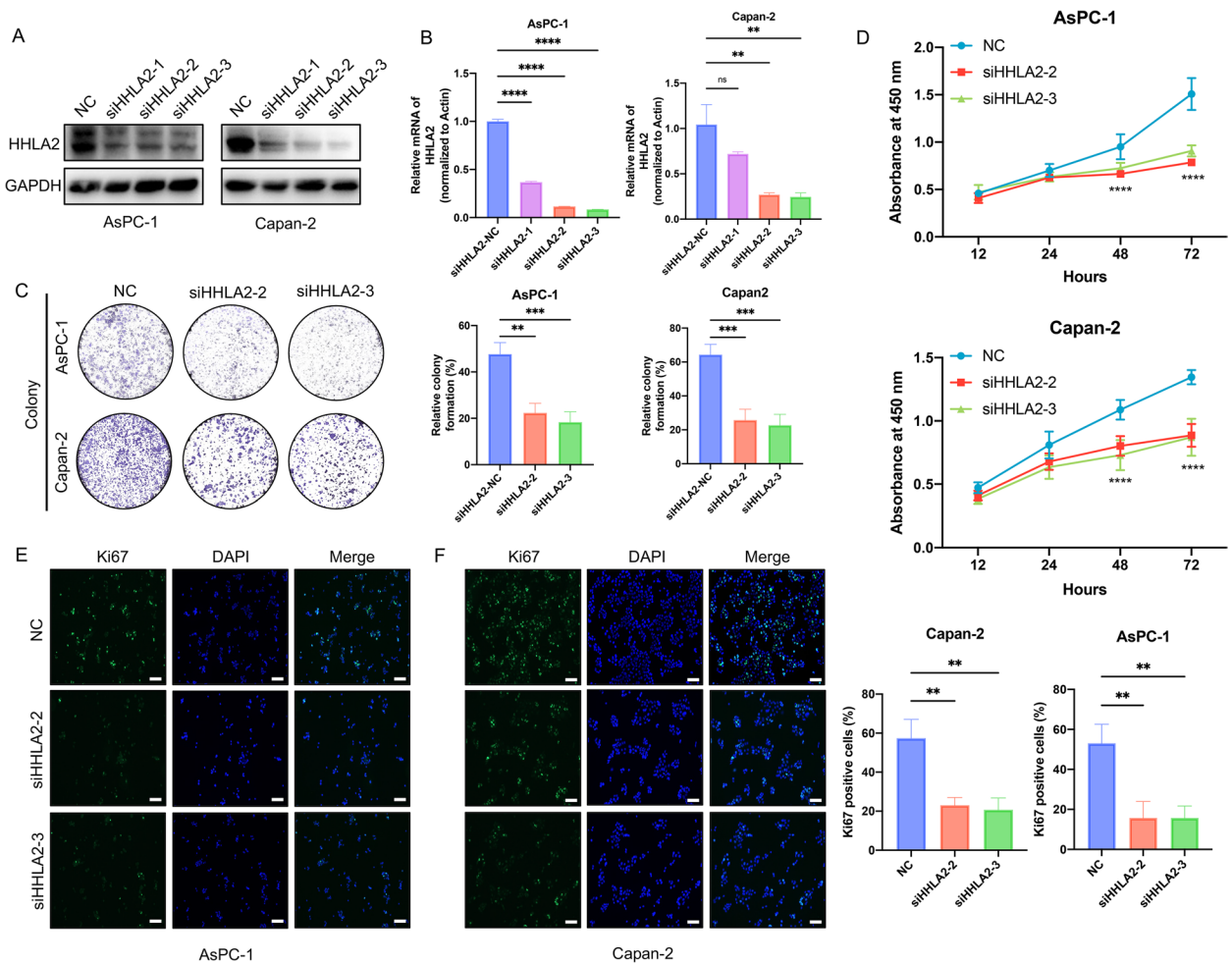
Zhou *et al. World Journal of Surgical Oncology*   (2024) 22:133

Page 8 of 13

Fig. 4 Effects of siHHLA2 on viability and proliferation of PC cells. **A** The relative expression level of protein of siHHLA2 in AsPC-1 and Capan-2. **B** The relative expression level of mRNA of siHHLA2 in AsPC-1 and Capan-2. The effect of siHHLA2-2 and siHHLA2-3 on the growth of PC cells was detected by colony formation assay (**C**), CCK-8 (**D**) and immunofluorescence staining. Scale bar: 100 μm (**E**&**F**). $^{*}p < 0.05$, $^{**}p < 0.01$, $^{***}p < 0.001$, $^{****}p < 0.0001$

The expressions of p-EGFR, p-MEK, p-ERK1/2, p-AKT and p-mTOR were all significantly decreased compared with NC group (Fig. 7C&D). These results suggested that knockdown of HHLA2 inactivated EGFR/MAPK/ERK and mTOR/AKT pathway.

Silencing of HHLA2 in PC cells inhibits M2 polarization of macrophages

Finally, effects of HHLA2 on polarization of TAM were examined. We performed the immune infiltration score for the TCGA database through CIBERSORT algorithm, and we calculated the spearman correlation coefficient of the B7 family genes with the immune invasion score to identify significantly correlated immune invasion scores (Fig. 8A). We ultimately observed a significant correlation between B7 family gene expression and immune invasion in TCGA-PAAD. TCGA and TIMER2.0 database showed that M2 macrophage infiltration was positively correlated with HHLA2 expression in PC (Fig. 8B&C). To further explore whether silencing of HHLA2 in PC cell lines was involved in the polarization of TAMs, siHHLA2 or NC was transfected into AsPC-1 and Capan-2 cells. The M0 macrophages were then incubated with conditional medium from NC and siHHLA2 cells for 48 h, and the expressions of M2 markers, CD163, CD206, Arg1 and IL-10 were detected by RT-qPCR. We found the expression levels of CD163, CD206, Arg-1 and IL-10 were significantly up-regulated in the cells of siHHLA2 NC transfected AsPC-1 and Capan-2 compared with M0 group; meanwhile, the expressions of the above markers were partially inhibited by the transfection of siHHLA2-1 and siHHLA2-2 in AsPC-1 and Capan-2 cells (Fig. 8D).
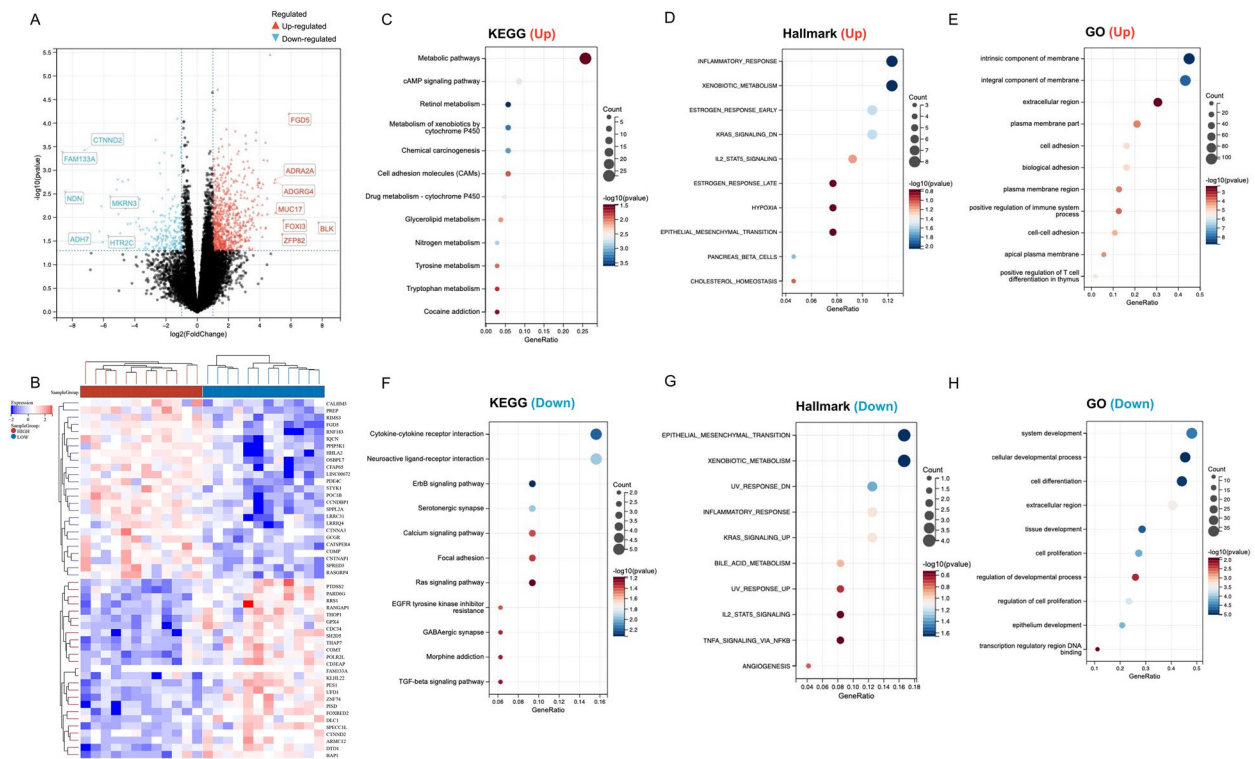
Fig. 5 Function enrichment analysis of HHLA2-related gene sets in PC. **A** Differentially expressed genes (DEGs) for high expression of HHLA2 vs. low expression of HHLA2 in PC were shown in the volcano plot, with red dots representing significantly up-regulated genes and blue dots representing significantly down-regulated genes in PC with high expression of HHLA2. **B** The heatmap exhibits the expression level. **C** Enrichment analysis for KEGG pathway of up-regulated genes. **D** Enrichment analysis for Hallmark pathway of up-regulated genes. **E** Enrichment analysis for GO term of up-regulated genes. **F** Enrichment analysis for KEGG pathway of down-regulated genes. **G** Enrichment analysis for Hallmark pathway of down-regulated genes. **H** Enrichment analysis for GO term of down-regulated genes

Conclusion

During the past decades, investigations on immune checkpoint therapy significantly changed the field of cancer treatment. B7 family is one of the most important co-signaling molecules, which is widely expressed in tumor cells and is closely related to tumor progression [23]. B7 family proteins positively or negatively regulate T cell function and are essential for maintaining immune regulation and self-tolerance. The B7 family is the most promising target for immunotherapy, either alone or in combination with other therapies. As a newly discovered member of the B7 family, HHLA2 is absent in most normal tissues, but is over-expressed in some malignant tumors [24]. In this study, we focused on the biological roles of HHLA2 in PC and the immunomodulatory effects of HHLA2 on macrophage polarization. We discovered that HHLA2 is over-expressed in PC and can inhibit the proliferation, migration and invasion of PC cells, and also block the M2 polarization of TAM through regulating EGFR/MAPK/ERK pathway.

HHLA2 overexpression has been reported to be associated with an increased risk of carcinogenesis. For example, results of a previous study suggested that HHLA2 is up-regulated in gallbladder cancer, and increased expression of HHLA2 may indicate poor prognosis [25]; moreover, the destiny of CD8^{+} TILs was also significantly reduced with increased expression of HHLA2 [26]. In the case of PC, the high expression level of HHLA2 not only reveals the occurrence, development, metastasis, prognosis and immune escape mechanism, but may also suggest that HHLA2 can be used as a potential target for immunotherapy of PC patients [27, 28].

In this study, the expression of B7 family member proteins in pancreatic cancer tissues and adjacent normal tissues were investigated by bioinformatics analysis using TCGA, GTEx and TIMER databases. Meanwhile, the clinical significance of HHLA2 in PC was further investigated; furthermore, the effects of HHLA2 on PC cell behaviors were also examined. We
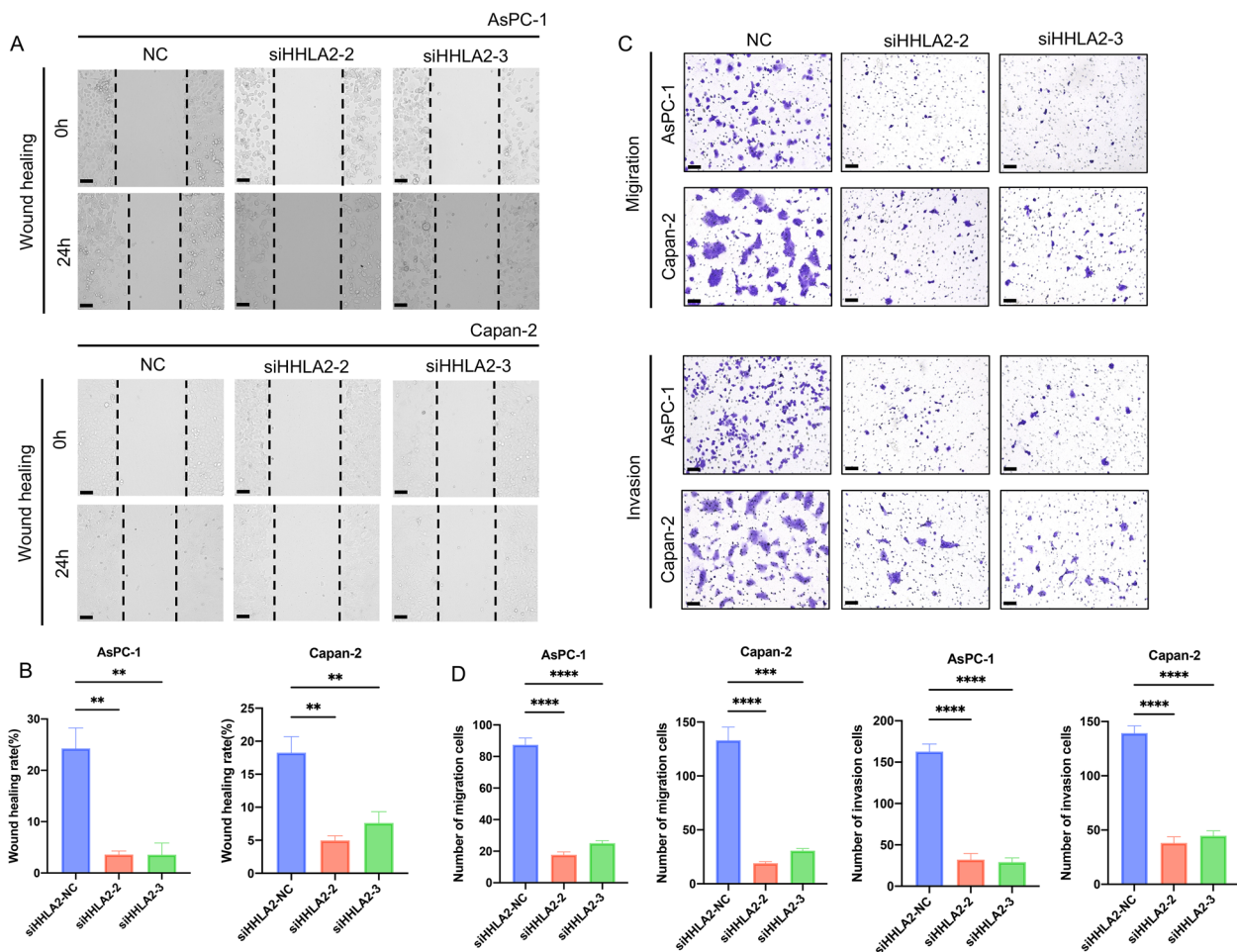
Zhou *et al. World Journal of Surgical Oncology*   (2024) 22:133

Page 10 of 13

Fig. 6 Effects of siHHLA2-2 and siHHLA2-3 on the invasion and migration. **A**&**B**, migration and invasion (**C**&**D**) of AsPC-1 and Capan-2 cells. Scale bar: 100 μm. $^{*}p<0.05$, $^{**}p<0.01$, $^{***}p<0.001$, $^{****}p<0.0001$

found that HHLA2 in over-expressed in PC tissues and cells, moreover, results of cell studies confirmed the oncogenic roles of HHLA2. Taken together, these results suggested that HHLA2 may regulate the growth and metathesis of PC cells, however, the underlying mechanism remains to be investigated.

Epithelial-mesenchymal transition (EMT) refers to the changes that occur in cells under certain physiological and pathological conditions. EMT plays an important role in cell embryonic development, organ differentiation, wound healing, and tumor metastasis [29]. Invasion and metastasis of pancreatic cancer are closely related to EMT [30–33]. Activation of the EGFR/MAPK/mTOR/AKT/ERK1/2 signaling pathway has been reported to promote cancer cell growth, survival, and metabolism [34]. Aberrant activation of the EGFR/MAPK/mTOR/AKT/ERK1/2 signaling pathway

occurs in a variety of human cancer cells [35]. EGFR is a tyrosine kinase-type receptor that is commonly activated or overexpressed in a variety of cancers, and the MAPK/ERK signaling pathway mediates the biological effects of EGFR activation [36, 37]. The AKT-mTOR signaling cascade is involved in several physiological and pathological processes, and mTOR is one of the downstream kinases of the AKT signaling pathway. In addition, activation of the EGFR/MAPK/mTOR/AKT/ERK1/2 signaling pathway in various cancers, such as glioblastoma, endometrial cancer, and prostate cancer can promote cancer cell invasion, metastasis, and drug resistance. In our study, we found that silencing of HHLA2 can inhibit the EMT process of pancreatic cancer cells, and the mechanism may be related to the regulation of EGFR/MAPK /mTOR/AKT/ERK1/2 signaling pathway.
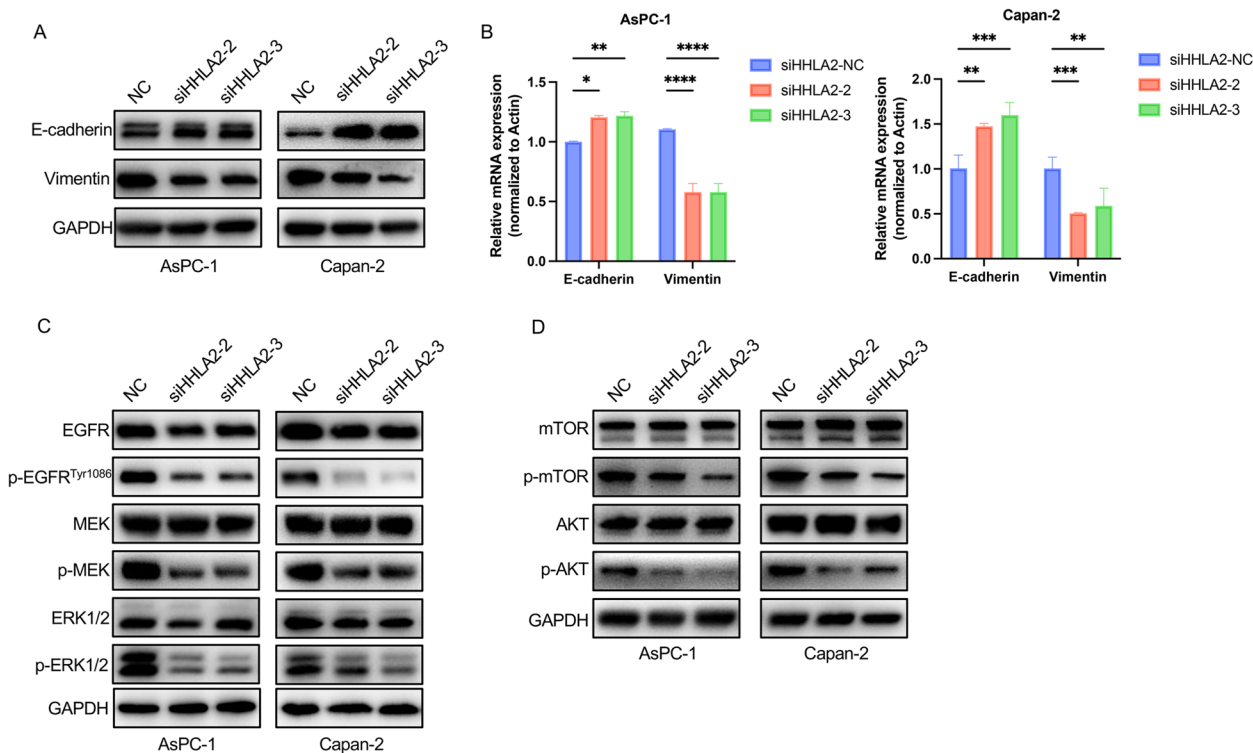
Zhou *et al. World Journal of Surgical Oncology*   (2024) 22:133

Page 11 of 13

Fig. 7 Effects of siHHLA2-2 and siHHLA2-3 on EGFR/MEK/ERK1/2/AKT/mTOR pathway in AsPC-1 and Capan-2 cells. **A**&**B** WB and RT-qPCRwere performed to evaluate the protein and mRNA levels of E-Cadherin and Vimentin expression after HHLA2 knockdown. **C** Knockdown of HHLA2 inhibited the activity of EGFR/MAPK/ERK signaling pathway in AsPC-1 and Capan-2 cells. **D** Knockdown of HHLA2 inhibited the activity of AKT/mTOR signaling pathway in AsPC-1 and Capan-2 cells. $^{*}p<0.05$, $^{**}p<0.01$, $^{***}p<0.001$, $^{****}p<0.0001$

Previously, most of the ideas for the treatment of cancer were focused on affecting the behaviors of the tumor cells. In recent years, the roles of tumor microenvironment has attracted more and more attentions. Tumor-associated macrophages (TAMs) refer to a type of macrophages that gather to the periphery of tumor tissues and undergo specific differentiation in the tumor microenvironment under the action of related chemokines [38]. Primitive macrophages (M0 type) can be polarized into M1 or M2 macrophages under different conditions [39]. TAMs are mostly M2 type, which promote tumor growth, invasion and metastasis by secreting a variety of active substances. At present, there are mainly two approaches for blocking tumor-associated macrophages: to inhibit the accumulation of monocytes/tumor-associated macrophages at the tumor site, or to affect the polarization of tumor-associated macrophages to the anti-tumor subtype. In our study, the tumor-infiltrating immune cell model showed that the level of HHLA2 was positively correlated with TAMs in PC, suggesting that HHLA2 was associated with TAMs. Also, we found that after silencing HHLA2 in AsPC-1 and Capan-2 cells, the expression of M2 macrophage markers were significantly decreased. These results indicated that the M2-type polarization of TAMs can be inhibited after silencing HHLA2. The current study also has limitations. HHLA2 is a member of the B7 family that expressed only in humans but not in mice, therefore, the current study only included human samples and human cell lines. In future study, the in vivo analysis may also be conducted by using humanized-mice models.

In conclusion, we found that the expression of HHLA2 is up-regulated in PC tissues, and silencing of HHLA2 can inhibit the proliferation, migration and invasion of PC cells. Meanwhile, silencing HHLA2 can block the EMT process and inhibit the invasion of PC cells, and its mechanism may be related to the regulation of mTOR/AKT and EGFR/MAPK/ERK signaling pathway. Finally, silencing of HHLA2 also inhibited the M2 polarization of TAMs. Our data may provide new evidence for targeting HHLA2 as a novel approach for the management of PC.
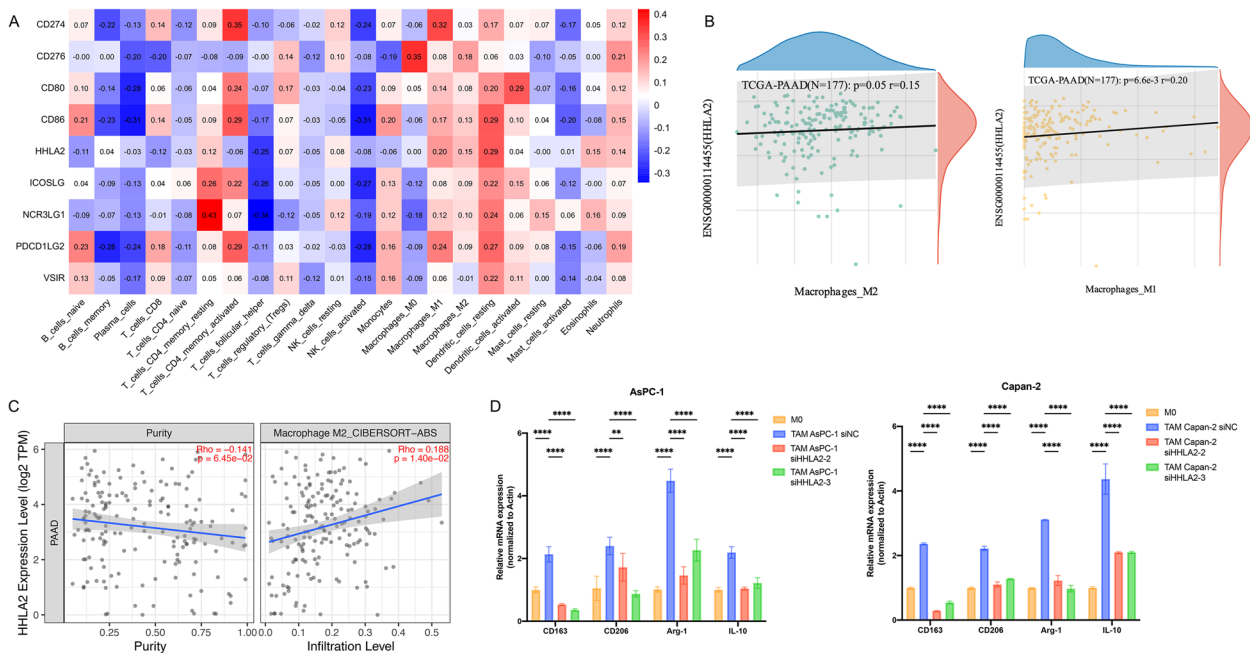
Fig. 8 Silencing HHLA2 in AsPC-1 and Capan-2 inhibited M2 polarization of TAMs. **A-C** TIMER2.0 and TCGA database suggested that M2 macrophage infiltration in pancreatic tissue was positively correlated with HHLA2 expression; **D** M0 macrophages and co-cultured TAMs expressed changes in the expression levels of M2-type macrophage markers. $^*p<0.05$, $^{**}p<0.01$, $^{***}p<0.001$, $^{****}p<0.0001$

Supplementary Information

The online version contains supplementary material available at https://doi.org/10.1186/s12957-024-03409-2.

Supplementary Material 1: Supplemental table. Relationship between HHLA2 and clinical features of patients with pancreatic cancer(a. 171 pancreatic cancer patients obtained from the TCGA database; b. Self-made pancreatic cancer tissue microarray).

Authors' contributions
SZ and ZW designed the study and drafted the manuscript. DZ, YF and SZ were responsible for the collection and analysis of the experimental data. ZW and XZ revised the manuscript critically for important intellectual content. All authors read and approved the final manuscript.

Availability of data and materials
No datasets were generated or analysed during the current study.

Declarations

Ethics approval and consent to participate
The study was approved by the Ethics Committee of Nanjing Drum Tower Hospital Clinical College of Jiangsu University. Signed written informed consents were obtained from the patients and/or guardians.

Consent for publication
Not applicable.

Competing interests
The authors declare no competing interests.

Author details
[1]Department of Gastroenterology, Nanjing Drum Tower Hospital Clinical College of Jiangsu University, No.321, Zhongshan Road, Nanjing 210008, China. [2]Department of Gastroenterology, Nanjing Drum Tower Hospital, The Affiliated Hospital of Nanjing University Medical School, Nanjing 210008, China. [3]State Key Laboratory of Holistic Integrative Management of Gastrointestinal Cancers, National Clinical Research Center for Digestive Diseases, Xijing Hospital of Digestive Diseases, Fourth Military Medical University, Xi'an 710032, China. [4]Department of Pathology, Nanjing Drum Tower Hospital, The Affiliated Hospital of Nanjing University Medical School, Nanjing 210008, China. [5]Department of Anesthesiology, The Affiliated Hospital of Xuzhou Medical University, No.99, Huaihai West Road, Xuzhou 221000, China.

References
1. Sung H, Ferlay J, Siegel RL, Laversanne M, Soerjomataram I, Jemal A, Bray F. Global Cancer statistics 2020: GLOBOCAN estimates of incidence and Mortality Worldwide for 36 cancers in 185 countries. CA Cancer J Clin. 2021;71:209–49.
2. Elsayed M, Abdelrahim M. The latest Advancement in Pancreatic Ductal Adenocarcinoma Therapy: a review article for the latest guidelines and Novel therapies. Biomedicines. 2021;9(4):389.
3. Siegel RL, Miller KD, Wagle NS, Jemal A. Cancer statistics, 2023. CA Cancer J Clin. 2023;73:17–48.
4. Chamma H, Smith J, Johnson L, Wang X. Activation of STING in the pancreatic tumor microenvironment: a novel therapeutic opportunity. Cancer Lett. 2022;538:215694.
5. Raghavan S, Brown E, White M, Black J. Microenvironment drives cell state, plasticity, and drug response in pancreatic cancer. Cell. 2021;184:6119–e613726.

Zhou *et al. World Journal of Surgical Oncology*   (2024) 22:133

Page 13 of 13

6. Balachandran VP, Green A, Robinson P, Taylor K. Identification of unique neoantigen qualities in long-term survivors of pancreatic cancer. Nature. 2017;551:512–6.

7. Abdel-Rahman O. Immune checkpoints aberrations and gastric cancer; assessment of prognostic value and evaluation of therapeutic potentials. Crit Rev Oncol Hematol. 2016;97:65–71.

8. Schwab C, Jones R, Miller S, Anderson A. Phenotype, penetrance, and treatment of 133 cytotoxic T-lymphocyte antigen 4-insufficient subjects. J Allergy Clin Immunol. 2018;142:1932–46.

9. Hingorani SR, Zheng L, Bullock AJ, Seery TE, Harris WP, Sigal DS, Braiteh F, Ritch PS, Zalupski MM, Bahary N, Oberstein PE, Wang-Gillam A, Wu W, Chondros D, Jiang P, Khelifa S, Pu J, Aldrich C, Hendifar AE. HALO 202: Randomized Phase II study of PEGPH20 plus Nab-Paclitaxel/ Gemcitabine versus Nab-Paclitaxel/Gemcitabine in patients with untreated, metastatic pancreatic ductal adenocarcinoma. J Clin Oncol. 2018;36:359–66.

10. Desai J, Fong P, Moreno V, Frentzas S, Meniawy T, Markman B, Voskoboynik M, Rahman T, Budha N, Wu J, Marlow J, Yang S, Calvo E, Martin-Liberal J. A phase 1/2 study of the PD-L1 inhibitor, BGB-A333, alone and in combination with the PD-1 inhibitor, tislelizumab, in patients with advanced solid tumours. Br J Cancer. 2023;128:1418–28.

11. Ni L, Dong C. New B7 Family checkpoints in Human cancers. Mol Cancer Ther. 2017;16:1203–11.

12. Ying H, Xu J, Zhang X, Liang T, Bai X. Human endogenous retrovirus-H long terminal repeat-associating 2: the next immune checkpoint for antitumour therapy. EBioMedicine. 2022;79:103987.

13. Mager DL, Hunter DG, Schertzer M, Freeman JD. Endogenous retroviruses provide the primary polyadenylation signal for two new human genes (HHLA2 and HHLA3). Genomics. 1999;59:255–63.

14. Flajnik MF, Tlapakova T, Criscitiello MF, Krylov V, Ohta Y. Evolution of the B7 family: co-evolution of B7H6 and NKp30, identification of a new B7 family member, B7H7, and of B7's historical relationship with the MHC. Immunogenetics. 2012;64:571–90.

15. Janakiram M, Shah UA, Liu W, Zhao A, Schoenberg MP, Zang X. The third group of the B7-CD28 immune checkpoint family: HHLA2, TMIGD2, B7x, and B7-H3. Immunol Rev. 2017;276:26–39.

16. Zhang W, Qiu Y, Xie X, Fu Y, Wang L, Cai Z. B7 family members in Lymphoma: promising novel targets for Tumor Immunotherapy? Front Oncol. 2021;11:647526.

17. Bolandi N, Derakhshani A, Hemmat N, Baghbanzadeh A, Asadzadeh Z, Afrashteh Nour M, Brunetti O, Bernardini R, Silvestris N, Baradaran B. The positive and negative Immunoregulatory Role of B7 Family: promising novel targets in gastric Cancer treatment. Int J Mol Sci. 2021;22(19):10719.

18. Bhatt RS, Berjis A, Konge JC, Mahoney KM, Klee AN, Freeman SS, Chen CH, Jegede OA, Catalano PJ, Pignon JC, Sticco-Ivins M, Zhu B, Hua P, Soden J, Zhu J, McDermott DF, Arulanandam AR, Signoretti S, Freeman GJ. KIR3DL3 is an inhibitory receptor for HHLA2 that mediates an alternative Immunoinhibitory pathway to PD1. Cancer Immunol Res. 2021;9:156–69.

19. Yan H, Qiu W, Koehne de Gonzalez AK, Wei JS, Tu M, Xi CH, Yang YR, Peng YP, Tsai WY, Remotti HE, Miao Y, Su GH. HHLA2 is a novel immune checkpoint protein in pancreatic ductal adenocarcinoma and predicts post-surgical survival. Cancer Lett. 2019;442:333–40.

20. Li Y, Lv C, Yu Y, Wu B, Zhang Y, Lang Q, Liang Z, Zhong C, Shi Y, Han S, Xu F, Tian Y. KIR3DL3-HHLA2 and TMIGD2-HHLA2 pathways: the dual role of HHLA2 in immune responses and its potential therapeutic approach for cancer immunotherapy. J Adv Res. 2023;47:137–50.

21. Zhou Q, Li K, Lai Y, Yao K, Wang Q, Zhan X, Peng S, Cai W, Yao W, Zang X, Xu K, Huang J, Huang H. B7 score and T cell infiltration stratify immune status in prostate cancer. J Immunother Cancer. 2021;9(8):e002455.

22. Shen W, Song Z, Zhong X, Huang M, Shen D, Gao P, et al. Sangerbox: a comprehensive, interaction-friendly clinical bioinformatics analysis platform. iMeta. 2022;1(3):e36.

23. Lv C, Han S, Wu B, Liang Z, Li Y, Zhang Y, Lang Q, Zhong C, Fu L, Yu Y, Xu F, Tian Y. Novel immune scoring dynamic nomograms based on B7-H3, B7-H4, and HHLA2: potential prediction in survival and immunotherapeutic efficacy for gallbladder cancer. Front Immunol. 2022;13:984172.

24. Koirala P, Roth ME, Gill J, Chinai JM, Ewart MR, Piperdi S, Geller DS, Hoang BH, Fatakhova YV, Ghorpade M, Zang X, Gorlick R. HHLA2, a member of the B7 family, is expressed in human osteosarcoma and is associated with metastases and worse survival. Sci Rep. 2016;6:31154.

25. Wei Y, Ren X, Galbo PM, Moerdler S, Wang H, Sica RA, Etemad-Gilbertson B, Shi L, Zhu L, Tang X, Lin Q, Peng M, Guan F, Zheng D, Chinai JM, Zang X. KIR3DL3-HHLA2 is a human immunosuppressive pathway and a therapeutic target. Sci Immunol. 2021;6(61):eabf9792.

26. Kula A, Dawidowicz M, Mielcarska S, Kiczmer P, Skiba H, Krygier M, Chrabańska M, Piecuch J, Szrot M, Robotycka J, Ochman B, Strzałkowska B, Czuba Z, Świętochowska E, Waniczek D. Overexpression and role of HHLA2, a Novel Immune Checkpoint, in Colorectal Cancer. Int J Mol Sci. 2023;24(6):5876.

27. Zhu Y, Chen J, Liu Y, Zheng X, Feng J, Chen X, Jiang T, Li Y, Chen L. Prognostic values of B7-H3, B7-H4, and HHLA2 expression in human pancreatic cancer tissues based on mIHC and spatial distribution analysis. Pathol Res Pract. 2022;234:153911.

28. Zhao R, Chinai JM, Buhl S, Scandiuzzi L, Ray A, Jeon H, Ohaegbulam KC, Ghosh K, Zhao A, Scharff MD, Zang X. HHLA2 is a member of the B7 family and inhibits human CD4 and CD8 T-cell function. Proc Natl Acad Sci U S A. 2013;110:9879–84.

29. Akhurst RJ. From shape-shifting embryonic cells to oncology: the fascinating history of epithelial mesenchymal transition. Semin Cancer Biol. 2023;96:100–14.

30. Di Giorgio E, Cortolezzis Y, Gualandi N, Agostini F, Rapozzi V, Xodo LE. NRF2 interacts with distal enhancer and inhibits nitric oxide synthase 2 expression in KRAS-driven pancreatic cancer cells. Biochim Biophys Acta Mol Cell Res. 2023;1871:119606.

31. Chien TL, Wu YC, Lee HL, Sung WW, Yu CY, Chang YC, Lin CC, Wang CC, Tsai MC. PNU-74654 induces cell cycle arrest and inhibits EMT progression in pancreatic Cancer. Med (Kaunas). 2023;59(9):1531.

32. Li S, Jiang F, Chen F, Deng Y, Huang H. Silencing long noncoding RNA LINC01133 suppresses pancreatic cancer through regulation of microRNA-1299-dependent IGF2BP3. J Biochem Mol Toxicol. 2023;17:e23534.

33. Su X, Lai T, Tao Y, Zhang Y, Zhao C, Zhou J, Chen E, Zhu M, Zhang S, Wang B, Mao Y, Hu H. miR-33a-3p regulates METTL3-mediated AREG stability and alters EMT to inhibit pancreatic cancer invasion and metastasis. Sci Rep. 2023;13:13587.

34. Rosenberg L, Yoon CH, Sharma G, Bertagnolli MM, Cho NL. Sorafenib inhibits proliferation and invasion in desmoid-derived cells by targeting Ras/MEK/ERK and PI3K/Akt/mTOR pathways. Carcinogenesis. 2018;39:681–8.

35. Su CC. Tanshinone IIA can inhibit MiaPaCa–2 human pancreatic cancer cells by dual blockade of the Ras/Raf/MEK/ERK and PI3K/AKT/mTOR pathways. Oncol Rep. 2018;40:3102–11.

36. Ren Y, Hong Y, He W, Liu Y, Chen W, Wen S, Sun M. EGF/EGFR promotes salivary adenoid cystic Carcinoma cell malignant neural Invasion via activation of PI3K/AKT and MEK/ERK Signaling. Curr Cancer Drug Targets. 2022;22:603–16.

37. Yang R, Li X, Wu Y, Zhang G, Liu X, Li Y, Bao Y, Yang W, Cui H. EGFR activates GDH1 transcription to promote glutamine metabolism through MEK/ERK/ELK1 pathway in glioblastoma. Oncogene. 2020;39:2975–86.

38. Xiang X, Wang J, Lu D, Xu X. Targeting tumor-associated macrophages to synergize tumor immunotherapy. Signal Transduct Target Ther. 2021;6:75.

39. Pan Y, Yu Y, Wang X, Zhang T. Tumor-Associated macrophages in Tumor Immunity. Front Immunol. 2020;11:583084.

Publisher's Note